Minimal model of relaxation in an associating fluid: Viscoelastic and dielectric relaxations in equilibrium polymer solutions

ARTICLE *in* THE JOURNAL OF CHEMICAL PHYSICS · DECEMBER 2006

Impact Factor: 2.95 · DOI: 10.1063/1.2378648 · Source: PubMed

2 AUTHORS:

Evgeny Stukalin
University of Chicago
26 PUBLICATIONS **624** CITATIONS

SEE PROFILE

Karl F. Freed
University of Chicago
657 PUBLICATIONS **16,415** CITATIONS

SEE PROFILE

Minimal model of relaxation in an associating fluid: Viscoelastic and dielectric relaxations in equilibrium polymer solutions

Evgeny B. Stukalin[a] and Karl F. Freed
The James Franck Institute, University of Chicago, Chicago, Illinois 60637

(Received 7 September 2006; accepted 6 October 2006; published online 13 November 2006)

Cluster formation and disintegration greatly complicate the description of relaxation processes in complex fluids. We systematically contrast the viscoelastic and dielectric properties for models of equilibrium polymers whose thermodynamic properties have previously been established. In particular, the monomer-mediated model allows chain growth to proceed only by monomer addition, while the scission-recombination model enables all particles to associate democratically, so that chain scission and fusion occur at the interior segments as well as at chain ends. The minimal models neglect hydrodynamic and entanglement interactions and are designed to explore systematically the competition between chemical reaction and internal chain relaxation and how this coupling modifies the dynamics from that of a polydisperse solution of Rouse chains with fixed lengths (i.e., "frozen" chains). As expected, the stress relaxation is nearly single exponential when the assembly-disassembly reaction is fast on the time scale of structural chain rearrangements, while multiexponential or nearly stretched exponential relaxation is obtained when this reaction rate is slow compared to the broad relaxation spectrum of almost unperturbed, nearly "dead" chains of intrinsically polydisperse equilibrium polymer solutions. More generally, a complicated intermediate behavior emerges from the interplay between the chemical kinetic events and internal chain motions. © *2006 American Institute of Physics*. [DOI: 10.1063/1.2378648]

I. INTRODUCTION

Molecular systems may self-assemble to form complex equilibrium structures that are subject to the directional interaction encoded in the intermolecular potentials of the assembling particles.[1,2] Beyond the basic problem of understanding the thermodynamic characteristics for this type of transition, there is a basic need for understanding the *dynamical properties* of associating fluids from a fundamental viewpoint.

Equilibrium polymerization is a common physical process in which monomers or n-mers form linear chains at equilibrium. The chains are "dynamic" in the sense that the polymers are constantly forming and disintegrating. These associating systems are also termed "living" polymer systems in contrast to systems where the mass distribution is arrested on experimentally accessible time scales and consequently where macroscopic properties are determined by an average over the frozen polydisperse mass distribution. Living polymer systems exhibit rather rich and nontrivial equilibrium and dynamic properties that vary greatly with the degree of aggregation. These properties include the molecular size distribution, the morphologies of the aggregates, and dynamic properties, such as the viscoelasticity, self-diffusion, and dielectric permittivity. Examples of reversible equilibrium aggregating systems include flexible linear macromolecules such as poly-α-methylstyrene,[3,4] giant micelles comprised of surfactant molecules,[5] some inorganic compounds (sulfur[6] and selenium[7]), and protein filaments[3,8] (actin filaments and microtubules). Association is known to determine the stability of micellar systems, ionic fluids, and nanoparticle dispersions. Aggregating systems provide important candidates for synthesis and molecular manipulation to produce complex structures with new properties.[3,9] However, our understanding of the impact of self-assembly on the macroscopic dynamic properties of aggregating systems is still quite limited.

Thermodynamic theory considers the time average properties of reversibly aggregating systems, such as the average number L of monomers in the chains, the fractions ϕ_1 of monomers in the associated state, and the temperature dependence of the time average of these quantities. The rate at which these aggregation-dissociation processes occur is evidently important for determining the dynamical properties of these fluids. Recent simulations have established the importance of the persistence of association in understanding the dynamic properties of aggregating polymer solutions at equilibrium,[10] and this phenomenon requires greater illumination. Cates and co-workers have recently addressed similar issues based on a model that incorporates phenomenological reptation concepts with a particular model for the reaction kinetics. Contact is made with this work below, and common features are found along with distinct differences.

Equilibrium polymerization actually connotes a family of models involving different constraints on the association-dissociation dynamics. The general classification scheme has been introduced by Tobolsky and Eisenberg, who pioneered the theory of equilibrium polymerization.[11] These *thermodynamic* models include the I model in which monomers only add to the chain ends in the presence of an "initiator" species

[a]Electronic mail: stukalin@uchicago.edu

that lowers the free-energy barrier for bond formation. We consider one model of an associating fluid that is similar to the I model in the sense that single monomers can add or dissociate at chain ends. This monomer-mediated[12] (MM) reaction model differs from the I model only in the absence of a chemical initiator. Another basic thermodynamic model is the FA or free-association model where all particles can associate and dissociate into chains without any constraint except the condition of thermodynamic equilibrium. Thus, the reaction kinetics of the FA model are identical to what has been called the scission-recombination (SR) mechanism.[5,12] The third basic model, the activated association model, requires that the monomers must be thermally "activated" before particles can be associated. This later situation occurs in sulfur where S_8 sulfur rings must break open due to thermal motions before chain formation can occur.[13] The present work confines itself to the extreme cases of the SR and MM models, which are identical or similar to the FA and I models, respectively, and are representations of the rather broad range of behaviors seen in equilibrium models.

The present paper describes initial steps in this direction by systematically treating the stress and dielectric relaxation in solutions of equilibrium polymers where hydrodynamic and entanglement interactions are neglected, interactions that become important phenomenologically in dilute and in concentrated high molecular weight solutions, respectively. However, the general trends that are described are believed to apply also to fluids having these more complex interactions. The main focus here is on the particular problem of how the cluster formation-disintegration process and the time scales governing the clustering dynamics modify the stress and dielectric relaxation processes from those of solutions of clusters having a fixed polydisperse mass distribution.

We provide a theoretical description of the influence on the dynamics of reversible aggregating systems of the coupling between chemical relaxation, due to chemical reactions that result in a change in chemical species, and internal relaxation, that arises from the structural rearrangements within chains of fixed lengths. The analysis uses a discrete chain molecular model and explicitly considers the viscoelastic properties and the dielectric relaxation. The general theory is applicable to a wide range of dynamic models since the relaxation is described in terms of the relaxation time distribution. However, because our focus is on understanding general trends emerging from this coupling, many illustrations of the general formulation use the analytically simplest Rouse model for the internal chain dynamics and two distinct kinetic models for the association/dissociation that correspond at equilibrium to the simplest FA and I models.[14] Assuming the independence of the chemical and structural relaxation processes, we derive analytical expressions for the viscoelastic and dielectric functions for an equilibrium system composed of self-associating linear macromolecules as a functions of polymer density, temperature, chain length, kinetic rate constants for the polymerization process, and interaction and geometric parameters of the bead-spring model, such as the monomeric friction coefficient and the mean-square end-to-end distance. In contrast to the independence of equilibrium properties to the reaction kinetics within the SR and MM models,[14] dynamic properties strongly depend on the mechanism of chemical relaxation that is dictated by the kinetics of self-association and disintegration.

Section II considers the stress relaxation function and dielectric permittivity in the presence of the reversible breaking and restoration of chains, focusing on the competition between chemical and structural relaxation processes. Calculations illustrate the equilibrium properties of polydisperse systems and the influence of chemical relaxation for two different mechanisms of polymerization corresponding to the SR and MM models. Section III presents the derivation of explicit general expressions and illustrations of general trends for the dynamical properties of living polymer systems, such as the complex viscosity and dielectric permittivity. Dynamic properties of equilibrium polymer systems are compared for MM model and SR model reaction kinetics. The models are analyzed both for slow and fast chemical relaxation dynamics in Sec. IV, and a comparison with the relaxation model of Cates is illustrated for Rouse-type chain dynamics. The Appendix presents the derivation of closed form analytical expressions for the contributions from individual chains to the viscoelastic and dielectric functions of living polymers with Rouse dynamics as well as those for the viscoelasticity of living and unbreakable chains in the reptation model.

II. STRESS RELAXATION FOR EQUILIBRIUM POLYMERS

In the absence of chemical relaxation (i.e., for "frozen" chains), the dynamics is described by models that are often represented in terms of a set of relaxation times τ_p for the "modes" p of relaxation. We consider this type of general expression for the complex frequency dependent viscosity and dielectric permitivity, but numerical calculations are illustrated for the simplest bead-spring Rouse model,[15–17] which describes dynamics in melts and concentrated solutions of nonentangled polymers. The Rouse model is used because of its greater analytical tractability and the need for a minimum number of parameters. As is well known, the Rouse model ignores the influence of hydrodynamic interactions and entanglements.

We consider a polydisperse system, where the distribution of chain lengths is determined by chemical equilibrium for the polymerization process and by the overall concentration ϕ of the solute. If the chemical relaxation is extremely slow on the experimental time scale, the reversible breaking and restoration of chains only results in a redistribution of mass between the aggregates, but the overall mass distribution is fixed by the condition of chemical equilibrium.[18] The simplest model for the chemical relaxation process posits that each association and dissociation event involves only one chemical bond in the linear chain and is characterized by two mean-field rate constants k_A and k_D for chain growth and decomposition, respectively. Both k_A and k_D are assumed, for simplicity, to be independent of chain length and configuration.

This minimal model is consistent with at least two alternative kinetic mechanisms for the polymerization/aggregation process.[5,12,19,20] The first is a monomer-mediated

kinetic scheme[12] (MM model) in which each chain can grow through a bimolecular reaction with a monomer or the chain can lose a monomer at the chain end. Only one end is considered to be the active site of a macromolecule. The second alternative mechanism is the scission-recombination scheme (SR model).[5,19] We consider the specific example of the SR model in which a chain may break with equal probability into two shorter chains at any site along its length, or two chains can recombine with one another to form a larger chain. These two reaction kinetic models can be described as

$$c_N \rightleftharpoons c_{N-1} + c_1, \quad \text{MM model}, \tag{1}$$

$$c_N \rightleftharpoons c_{N'} + c_{N''}, \quad \text{SR model}, \tag{2}$$

where $N=N'+N''$

The equilibrium chain length distribution has been obtained analytically for the model of Eq. (2) after treating the chain length N as continuous parameter.[5,21] The equilibrium number density for chains of length N is obtained as the exponential distribution,

$$c_N = \frac{\phi}{L^2}\exp(-N/L), \tag{3}$$

where the average polymer length is $L=(\phi K_{\mathrm{eq}}/2)^{1/2}$ with $K_{\mathrm{eq}}=k_A/k_D$ the equilibrium constant for the addition of a monomer and $\phi=\Sigma_N N c_N$ is the total monomer density. The monomer-mediated polymerization reaction scheme also produces an exponential equilibrium distribution when L is not very small.[20] However, here the distribution is found by treating N as a discrete variable,[12]

$$c_N = \frac{1}{K_{\mathrm{eq}}}\left[\frac{1+2\phi K_{\mathrm{eq}}-\sqrt{1+4\phi K_{\mathrm{eq}}}}{2\phi K_{\mathrm{eq}}}\right]^N \simeq \frac{\phi}{L^2}\exp(-N/L), \tag{4}$$

where $L=2\phi K_{\mathrm{eq}}(\sqrt{1+4\phi K_{\mathrm{eq}}}-1)^{-1}\simeq(\phi K_{\mathrm{eq}})^{1/2}$ with K_{eq} defined as above. Using a discrete representation, both mechanisms are found to yield the same equilibrium chain length distribution $c_N=c_1 q^{N-1}$, where $q=1-1/L$. Note that this distribution does not apply for the activated A model and the living I polymerization model with *initiator* present because additional thermal activation and chemical initiation steps can alter the variation of L with ϕ and the sharpness of the polymerization transition. For living polymerization systems, the average polymer length L scales nearly linear with ϕ above the "critical polymerization concentration" defined as the value of ϕ^* at which no polymers are present in a solution ($L=1$) at a fixed concentration of chemical initiator. This behavior contrasts with that of the free-association model where the polymerization transition is extremely broad and L varies as $\phi^{1/2}$.[14] When the living polymerization is chemically initiated, the equilibrium *mass* distribution Nc_N, which is relevant for averaging the dynamic functions, is given by $Nc_N^{\mathrm{liv}}=(N+2)Cq^{N+2}$, and only slightly differs from the distribution Nc_N described in Eq. (4) for L large enough. Also the relation between the "exponential" factor q and the average polymer length L is different.[14]

A. Dynamic properties of polydisperse systems of frozen chains

The polymer contribution to the relaxation modulus for a system of frozen chains with exponential polydispersity is evaluated by summing over the normal modes for the collective motions and by averaging over the equilibrium polymer distribution,[15,22]

$$G(t) = \frac{1}{L^2}\sum_{N=1}^{+\infty} N q^{N-1} G_N(t) = \frac{\rho RT}{M_0 L^2}\sum_{N=1}^{+\infty}\sum_{p=1}^{N-1} q^{N-1}\exp(-2t/\tau_p). \tag{5}$$

Here $G_N(t)=\rho RT/M\Sigma_{p=1}^{N-1}\exp(-2t/\tau_p)$ is the relaxation modulus for chains of fixed length N, M and M_0 are the molecular weights of a polymer and monomer, respectively, ρ is the mass density of polymers, and the τ_p ($p=1,\ldots,N-1$) are the normal mode relaxation times. Attention here is restricted to a minimal model for the dynamics of associating fluids. In order to elucidate general trends arising from the coupling between particle association-dissociation and chain relaxation, this section illustrates these trends for the simplest Rouse model where the τ_p are known analytically as

$$\tau_p = \frac{\zeta_0 b^2}{12 k_B T}\sin^{-2}\left(\frac{\pi p}{2N}\right). \tag{6}$$

The prefactor $L^{-2}=\Sigma_{N=1}^{+\infty} N q^{N-1}$ in Eq. (5) arises from the normalization condition for averaging over the equilibrium distribution. Section IV describes an application in which a reptation model is used for the τ_p, while other models for the chain relaxation times may be substituted in Eq. (5).

The Rouse model does not apply for the monomer contribution to Eq. (5), so it is necessary to specify this quantity. For simplicity, the monomer contribution to the viscoelastic function is taken as identical to that of a solvent molecule, and the contribution of monomers and solvent is omitted from the dynamical properties to focus on the response of the aggregates. It is also evident that short chains are not Gaussian, and strictly speaking the Rouse formula of Eq. (6) is inapplicable for small N. However, the equilibrium weight density distribution $M_0 N c_N$ is maximum at the average polymer length L. Hence, if L is not small, the error in using Eq. (6) is minimal because most of the contributions to the relaxation modulus arise from chains whose lengths are near the maximum of the weight density distribution. Again, these approximations are consistent with our focus on general trends, and more detailed models are readily considered by substituting the appropriate τ_p.

The viscoelastic functions are obtained similarly. For example, the zero-shear viscosity $\eta_{0,N}$ for chains of fixed length N in the Rouse model is

$$\eta_{0,N} = \frac{\rho N_A \zeta_0 b^2}{36M}(N^2-1) \simeq \frac{N_A \zeta_0 b^2}{36 M_0}\rho N, \tag{7}$$

where N_A is Avogadro's number, ζ_0 is the monomer friction coefficient, b is the effective length of a segment, and M_0 is the molecular weight of a monomer. Averaging over the ex-

ponential chain length distribution (this time expressed with a continuous distribution) leads to

$$\eta_0 = \phi^{-1} \int_0^\infty N c_N \eta_{0,N} dN = 2\eta_{0,L}, \tag{8}$$

where L is the average chain length.

B. Associating fluids with reversible chemical dynamics

When the chemical relaxation induced by the bond breakage and reformation reactions is not slow on the time scales of measurements, the effect of the chemical dynamics cannot be described solely through an average over the equilibrium distribution of chain lengths as in Eq. (5). Stress relaxation may thus occur either via diffusive motion of individual chains or due to an "evaporation-condensation" mechanism arising from mass transfer between chains that takes place by virtue of the association-dissociation events.

We assume that each normal mode p of chain motion may relax either due to the dynamics of a chain of fixed length or because of a chemical reaction that changes the chain length. Both of these relaxation processes are taken to be independent, implying that the effective relaxation rate $1/\tau_{\text{eff}}$ for stress relaxation may be estimated as if these processes occur in parallel, i.e., as the harmonic average $1/\tau_{\text{eff}} = 1/\tau_p' + 1/\tau_c$, where $1/\tau_p' = 2/\tau_p$ is the rate of structural relaxation for mode p in an unbreakable chain [see Eq. (5)]. When τ_c is comparable with the longest structural relaxation times τ_p, the efficient mechanism for stress relaxation is determined by a coupling between the two types of system rearrangements. Given this assumption of independence, the shear relaxation modulus $G_c(t)$ is described by

$$G_c(t) = \frac{1}{L^2} \sum_{N=1}^{+\infty} N q^{N-1} G_{c,N}(t)$$

$$= \frac{\rho RT}{M_0 L^2} \sum_{N=1}^{+\infty} \sum_{p=1}^{N-1} q^{N-1} \exp(-2t/\tau_p) \exp(-t/\tau_c), \tag{9}$$

where τ_c is the characteristic time for the chemical reaction (1) or (2) and where τ_c depends on N in a manner to be determined below. Equation (9) clearly behaves properly in the limit that τ_c becomes infinite and the chains have fixed lengths.

The stress relaxation for an equilibrium polydisperse system with very rapid, monomer-mediated reaction kinetics, $\tau_c < \tau_p$ for all p, is exponential over the whole time scale t. Polydispersity does not destroy the exponential dependence since the lifetime τ_c of chains is practically independent of their lengths (see next section). The stress relaxation for an equilibrium polydisperse system with scission-recombination reaction kinetics is almost exponential for small τ_c. Polydispersity slightly influences the stress relaxation decay function since the lifetime τ_c depends on chain length ($\tau_c \sim N^{-1}$) (Ref. 23) (see below). Thus, as τ_c changes from large to small values, the relaxation spectrum changes from nonexponential to exponential. The complex viscosity $\eta_c^* = \eta_c' - i\eta_c''$ is related to the shear relaxation modulus and can be obtained through Fourier-Laplace transformation as $\eta_c^*(\omega) = 1/(i\omega) \int_0^\infty \exp(-i\omega t) G_c(t) dt$.

C. Dielectric relaxation

The complex dielectric permittivity $\varepsilon^* = \varepsilon' - i\varepsilon''$ of equilibrium associating systems is found similarly. We consider polymers whose dipoles are parallel to the chain contour (A-type), whereupon the dielectric relaxation is determined by the first derivative of the normalized time correlation function for the end-to-end vector $R(t)$,[15,24,25]

$$\varepsilon^*(\omega) = \varepsilon_\infty - \frac{1}{L^2} \sum_{N=1}^{+\infty} N q^{N-1} \left\{ \Delta\varepsilon \int_0^\infty \exp(-i\omega t) \frac{d}{dt} \times \left[\frac{\langle R(t)R(0) \rangle}{\langle R^2 \rangle} \right] dt \right\}. \tag{10}$$

Here, ε_∞ is the high frequency limit of the dielectric constant, and $\Delta\varepsilon$ is the relaxation strength which for A-type chains is related to the mean-square end-to-end distance $\langle R^2 \rangle$, the molecular weight M, and the solute concentration ρ,[24,25]

$$\Delta\varepsilon = \left(\frac{4\pi N_A \mu^2 F}{3k_B T} \right) \left(\frac{\rho \langle R^2 \rangle}{M} \right), \tag{11}$$

where μ is the dipole moment per unit contour length, and F is the ratio of internal and external electric fields.

For a monodisperse system following Rouse dynamics, the time correlation function in Eq. (10) is given by

$$\frac{\langle R(t)R(0) \rangle}{\langle R^2 \rangle} = \frac{8}{\pi^2} \sum_{p=1}^{N-1} \frac{1}{p^2} \exp(-t/\tau_p) \quad (p \text{ odd}). \tag{12}$$

In the presence of the reversible breaking-restoration of chains, the time correlation function is modified in a similar fashion as the stress relaxation, and the Rouse model yields the contribution from chains of fixed length N as

$$\left[\frac{\langle R(t)R(0) \rangle}{\langle R^2 \rangle} \right]_c = \frac{8}{\pi^2} \sum_{p=1}^{N-1} \frac{1}{p^2} \exp(-t/\tau_p) \times \exp(-t/\tau_c) \quad (p \text{ odd}). \tag{13}$$

Substituting Eq. (13) into Eq. (10) yields our description for polydisperse equilibrium aggregating systems, namely,

$$\varepsilon^*(\omega) = \varepsilon_\infty + \frac{1}{L^2} \sum_{N=1}^{+\infty} N q^{N-1} \Delta\varepsilon \times \left\{ \frac{8}{\pi^2} \sum_{p=1}^{N-1} \frac{1}{p^2} \frac{\tau_p^{-1} + \tau_c^{-1}}{\tau_p^{-1} + \tau_c^{-1} + i\omega} \right\} \quad (p \text{ odd}). \tag{14}$$

D. Chain scission relaxation times

The reaction schemes in Eqs. (1) and (2) produce infinite sets of coupled nonlinear kinetic equations (see below) with a broad range of characteristic relaxation times. Thus, a number of different approaches exist for estimating the characteristic times of reactions for these aggregating systems. This

difference depends, in part, on the manner in which the system may be perturbed, e.g., by a transition to nonequilibrium state following a c-jump or T-jump process, i.e., by sudden changes in concentration or temperature, respectively, or by an equilibrium fluctuation that implies a small instantaneous perturbation. The mean lifetime τ_c is defined as the characteristic time necessary for the system to relax after the perturbation is applied. The calculation of characteristic times for chemical relaxation becomes simplified for systems close to equilibrium where the chemical reaction dynamics is described by a system of coupled linear ordinary differential equations. Cates and co-workers have estimated relaxation times for both concentration and temperature jumps in the scission-recombination model,[21] while others have considered the relaxation based on a simplified treatment of the rate equations.[12,23] We focus on the response to concentration fluctuations as more indicative of the dynamics in equilibrium aggregating systems, especially when considering the relaxation for chains of particular sizes since this type of relaxation process enables defining a size dependent relaxation time.

The rate equations for the MM model reaction scheme can be expressed as the system of nonlinear differential equations,

$$\frac{dc_1}{dt} = -2k_A c_1^2 - k_A c_1 \sum_{j=2}^{\infty} c_j + 2k_D c_2 + k_D \sum_{j=3}^{\infty} c_j,$$
$$\frac{dc_j}{dt} = -(k_A c_1 + k_D) c_j + k_A c_1 c_{j-1} + k_D c_{j+1}, \quad j > 1, \tag{15}$$

where k_A is the association rate constant, k_D is the dissociation rate constant, and $K_{\mathrm{eq}} = k_A/k_D$ is the equilibrium constant. We omit an initial initiation step, for simplicity, in order to have the minimum number of adjustable parameters. There is no difficulty in extending the analysis to more elaborate kinetic models involving activation or initiation steps.[14] The factors of two in the first of equation (15) arise because the reaction of two monomers to produce a dimer consumes two chains of size $j=1$, while the decomposition of a dimer yields two monomers. The equilibrium distribution over cluster sizes may readily be determined by setting the left hand side of Eqs. (15) to zero, leading to $c_{j,0} = c_{1,0} q^{j-1}$, where $q = k_A c_{1,0}/k_D \leqslant 1$, and $c_{j,0}$ and $c_{1,0}$ are equilibrium concentrations of j-mers and monomers, respectively. The absolute values of the equilibrium concentrations $c_{j,0}$ are determined by the total polymer density through the mass conservation condition $\phi = \Sigma j c_j$.

The dynamical response to small perturbations in the equilibrium concentrations of each cluster is described by the deviations $\delta c_j(t) = c_j(t) - c_{j,0}$. Substituting the preceding expression for $c_i(t)$ into Eqs. (15), using the properties of the equilibrium solution, and also assuming that the perturbations $\delta c_j(t)$ are small, Eq. (15) reduces to a set of linearized equations governing the chemical dynamics near equilibrium,

$$\frac{1}{k_D}\frac{d\delta_1}{dt} = -\{4q + q^2/(1-q)\}\delta_1 + (2-q)\delta_2 + (1-q)\sum_{j=3}^{\infty} \delta_j,$$
$$\frac{1}{k_D}\frac{d\delta_j}{dt} = -(1+q)\delta_j + q\delta_{j-1} + \delta_{j+1} + q^{j-1}(1-q)\delta_1. \tag{16}$$

Numerical solutions of Eq. (16) can only be obtained after truncating the equations by introducing a maximal cluster size N_m, such that the equilibrium concentration $c_{N_m,0}$ is negligible for clusters of size N_m and greater. Then, the rate equations for δ_j $(j=1,\ldots,N_m)$, consistent with the mass conservation condition, reduce to

$$\frac{1}{k_D}\frac{d\delta_1}{dt} = -\{4q + q^2(1-q^{N_m-2})/(1-q)\}\delta_1 + (2-q)\delta_2 + (1-q)\sum_{j=3}^{N_m} \delta_j,$$
$$\frac{1}{k_D}\frac{d\delta_j}{dt} = -(1+q)\delta_j + q\delta_{j-1} + \delta_{j+1} + q^{j-1}(1-q)\delta_1,$$
$$\frac{1}{k_D}\frac{d\delta_{N_m}}{dt} = q\delta_{N_m-1} - \delta_{N_m} + q^{N_m-1}\delta_1. \tag{17}$$

Equations (16) are the limiting case of Eqs. (17) when N_m approaches infinity.

In general, the solution to the finite system of Eqs. (17) can be represented in terms of the fundamental solutions as

$$\delta_j(t) = \sum_{i=1}^{N_m} a_i u_{ij} \exp(-\mu_i t), \tag{18}$$

where u_{ij} is the jth component the ith eigenvector $\mathbf{u}_i = (u_{i1},\ldots,u_{iN_m})$ for the linearized system of equations, $-\mu_i$ are the corresponding eigenvalues that must be nonpositive, and a_i are constants that depend on the initial conditions for the concentration fluctuations. Due to the constraint of mass conservation, one eigenvalue vanishes, say, $\mu_{N_m}=0$, and the corresponding coefficient must be set as $a_{N_m} \equiv 0$ too, in order that the system is fully relaxed back to equilibrium in the large time limit.

We define a mean lifetime τ_c for each individual cluster c_k $(1 \leqslant k \leqslant N_m)$ by introducing a local perturbation $\delta_j(0)$ as the initial concentration fluctuation, such that the initial changes differ from zero only for those "reactants" involved into the rate equation for clusters of a specific size k, namely, for three "adjacent" clusters δ_k, $\delta_{k\pm1} \neq 0$ and the monomers $\delta_1 \neq 0$, while all other initial deviations from equilibrium concentrations are assumed to vanish, $\delta_j(0) = 0 (j \neq 1, k, k\pm1)$. The mass conservation condition for this choice of initial perturbations implies that only three of the $\delta_j(0)$ are independent, i.e., mass conservation implies $k\delta_k(0) + (k-1)\delta_{k-1}(0) + (k+1)\delta_{k+1}(0) + \delta_1(0) = 0$. Given the freedom of choice for k different from either 1 or N_m, we set $\delta_1(0)=0$ and take $\delta_{k-1} = \delta_{k+1} = -\delta_k/2$, so that the response only involves the single parameter δ_k. For $k=1$, we set $\delta_2 = -\delta_1/2$, while for $k=N_m$, $\delta_1 = \delta_{N_m-1} = -\delta_{N_m}$ is chosen. The truncated

linear set of ordinary differential equations may be solved numerically for each k using these initial conditions defining the local concentration fluctuations. The solutions are used to define characteristic relaxation times.

The characteristic time constant $\tau_c(k)$ for each cluster k and for the above choices of zero time perturbations $\delta_j(0)$ is naturally determined as a linear combination of reciprocal eigenvalues $-\mu_i^{-1}$,

$$\tau_c(k) = \frac{1}{\delta_k(0)} \int_0^\infty \delta_k(t)dt = \frac{1}{\delta_k(0)} \sum_{i=1}^{N_m-1} u_{ki}\mu_i^{-1}a_{ik}. \tag{19}$$

Thus, a matrix τ_c can be defined whose diagonal elements are the $\tau_c(k)$,

$$\|\tau_c(k)\| = U^T(\mu)^{-1}A, \tag{20}$$

where $U^T=\|u_{ij}\|^T$ is the transpose of the eigenvector matrix, $(\mu)^{-1}=\|\mu_i^{-1}\|$ is a diagonal matrix whose elements are the reciprocal of the eigenvalues, and $A=\|a_{ij}\|$ is a matrix that may be determined from the $t=0$ conditions for the kth set of concentration fluctuations for the clusters c_j $(j=1,\ldots,N_m)$ when the concentration of the cluster of a size k is perturbed locally. The initial conditions imply that $\delta_j^k(0)=\Sigma_{i=1}^{N_m}u_{ji}a_{ik}$, and hence, the factor of $\delta_k(0)$ cancels between numerator and denominator of Eq. (19), making $\tau_c(k)$ independent of $\delta_k(0)$.

Explicit numerical calculation of Eq. (18) for the characteristic relaxation times following small concentration fluctuations shows the $\tau_c(k)$ to be almost independent of the cluster size k and weakly dependent on the total polymer density. Only the monomers relax more quickly than the other species. The cutoff N_m has been chosen in the numerical calculations, such that the equilibrium properties for infinite N_m are reproduced with good accuracy. Beginning from dimers $j\geqslant 2$, the lifetimes for all cluster sizes are approximated quite well by the constant $\tau_c(j)=(2k_D)^{-1}$, a result consistent with a rough analysis of the rate equations by Milchev.[12] Indeed, neglecting the last two terms in Eq. (15) containing $c_{j\pm1}$ produces the simplified rate equation $dc_j/dt=-k_D(1+q)c_j$, which yields the characteristic time $1/\tau_c=k_D(1+q)=k_D(2-1/L)$.[12] For sufficiently large L, Milchev's estimate is close to that from our numerical analysis of $1/\tau_c(j)\simeq 2k_D$. This relaxation time is explained by the fact that "cluster" reactions are local and may occur only at the chain ends, so $\tau_c(j)$ is independent of chain length.

It appears that an analytical solution to the rate equations for the scission-recombination mechanism can only be found in the continuum limit. Characteristic times for scission-recombination reactions have been obtained in an elegant analysis by Cates and co-workers for the time evolution following a small c-jump perturbation from equilibrium,[21,26,27]

$$\tau_c = \frac{1}{k_D(2L+N)}. \tag{21}$$

This result for the lifetime τ_c is again as expected since a chain of size N has N possible reaction sites for bond breakage and hence has N-times larger probability to break than a chain in the monomer-mediated kinetic model. Thus, a qualitatively different chain length dependence of the relaxation times emerges for the MM and SR aggregation mechanisms. The weak dependence or practical independence on N for the MM model contrasts with the inverse proportionality to N in the SR model.

III. VISCOELASIC PROPERTIES AND DIELECTRIC RELAXATION

The complex viscosity is readily derived from the relaxation modulus in terms of the set of relaxation times τ_p. One benefit of using the Rouse model for illustrating the theory is the fact that the expression for the complex viscosity may be evaluated in closed form using contour integration (see Appendix for details). Hence, calculations for equilibrium polymerization systems can be performed with a single summation, rather than the double summation required when using, for example, a Zimm model for the chain relaxation times. The viscoelastic functions are affected by chemical dynamics, and the resultant functions are derived for the Rouse and reptation models. All expressions for the reptation model are presented in the Appendix, while the viscoelastic functions for Rouse dynamics are detailed in the present section.

The final closed form expression for the contribution to the complex viscosity from chains of particular length N following Rouse-type dynamics but affected by the reaction kinetics is obtained from the Appendix as

$$\eta^*_{c,N}(\omega_r) = \frac{\rho N_A \zeta_0 b^2}{24M_0}\left[\frac{\coth(2N \operatorname{arcsinh}\sqrt{\lambda_N + i\omega_r})}{\sqrt{\lambda_N+i\omega_r}\sqrt{1+\lambda_N+i\omega_r}} - \frac{1}{2N}\left(\frac{1}{\lambda_N+i\omega_r}+\frac{1}{1+\lambda_N+i\omega_r}\right)\right], \tag{22}$$

where $\omega_r=\kappa\omega$ is the reduced frequency, $\lambda_N=\kappa\tau_c^{-1}$ is the dimensionless characteristic time for the chemical reaction,

$$\kappa = \frac{\zeta_0 b^2}{24k_BT} = \frac{\pi^2}{8}\tau_0, \tag{23}$$

and τ_0 is the Rouse relaxation time constant. Alternatively, λ_N can be expressed using the ratio of the longest structural relaxation time $\tau_R=\tau_0N^2$ to τ_c, both N dependent,

$$\lambda_N \simeq \frac{\pi^2}{8N^2}\frac{\tau_R}{\tau_c}. \tag{24}$$

The final expression for the complex viscosity involves an average over the mass distribution $\eta_c^*(\omega_r)=L^{-2}\Sigma_{N=1}^{\infty}Nq^{N-1}\eta^*_{c,N}(\omega_r)$.

For frozen chains, $\lambda_N=0$, and the frequency dependent viscosity reduces to that for the Rouse model. It is interesting to compare the expression for $\eta_N^*(\omega)$ in Eq. (22) with the phenomenological model of Blizard,[28] who considers molecules as springs moving in a viscous medium with "spring constant" $3k_BT/qb^2$ (q is the number of subunits) and introduces a constant viscous coupling per unit length to the surrounding medium (equivalent to the introduction of a monomeric friction coefficient ζ_0).[28] The frequency dependent viscosity $\eta^*=G^*/(i\omega)$ in this representation is given by

$$\eta_N^*(\omega) = (C_1/M)[\sqrt{(iC_2M^2/\omega)}\coth\sqrt{iC_2M^2\omega}-1], \tag{25}$$

where C_1 and C_2 are unspecified constants. Equations (22) and (25) with $\lambda_N=0$ are similar but not identical. In the low

frequency limit, the two formulas are equivalent, and the direct comparison of these equations leads to the following parameter mapping: $C_1=\rho RT/2$ and $C_2=\zeta_0 b^2/6M_0k_BT$. At high frequencies, the Blizard equation yields the limiting real and imaginary complex viscosities $\eta'=\eta''=1/2C_1(C_2/\omega)^{1/2}$ as equal, while the asymptotic limits obtained using the Rouse model are different (see below). However, within a relatively wide range of ω, the continuous "Rouse-type" Blizard model and our analytical representation for the discrete version of the classical bead-spring model are in close agreement. Differences appear only for very high frequencies.

Separating the viscoelastic function into real and imaginary parts leads to

$$\eta'_{c,N}(\omega_r)=\frac{\rho N_A\zeta_0 b^2}{48M_0}\left[f_\eta(z^+)+f_\eta(z^-)-\frac{1}{N}\left(\frac{\lambda_N}{\lambda_N^2+\omega_r^2}+\frac{1+\lambda_N}{(1+\lambda_N)^2+\omega_r^2}\right)\right], \tag{26}$$

$$\eta''_{c,N}(\omega_r)=\frac{\rho N_A\zeta_0 b^2}{48M_0}\left[i\{f_\eta(z^+)-f_\eta(z^-)\}-\frac{\omega_r}{N}\left(\frac{1}{\lambda_N^2+\omega_r^2}+\frac{1}{(1+\lambda_N)^2+\omega_r^2}\right)\right], \tag{27}$$

where $z^\pm$ are given by

$$z^\pm=\lambda_N\pm i\omega_r, \tag{28}$$

and the functions

$$f_\eta(z^\pm)=\frac{\coth(2N\,\mathrm{arcsinh}\,\sqrt{z^\pm})}{\sqrt{z^\pm}\sqrt{1+z^\pm}}. \tag{29}$$

The average over the equilibrium chain length distribution [see Eqs. (8) and (9)] can be evaluated numerically, but some estimates are derived here. It is instuctive to compare the zero-shear viscosity $\eta_{c,0}$ of a polydisperse system with an exponential mass distribution for both kinetic reaction mechanisms with the "normalized" contribution $\eta_{c,0,L}$ from a monodisperse system of chains with length L. For $\tau_c\to\infty$, the chemical dynamics is irrelevant, and $\eta_0\simeq 2\eta_{0,L}$ [see Eq. (8)]. When $\tau_c\to 0$, the average zero-shear viscosity of the polydisperse system is

$$\eta_{c,0}=\frac{1}{L^2}\sum_{N=1}^{+\infty}Nq^{N-1}\eta_{c,0,N}=\frac{\rho RT}{M_0L^2}\sum_{N=1}^{+\infty}q^{N-1}(N-1)\tau_c. \tag{30}$$

Because τ_c is practically N independent for monomer-mediated kinetics, $\eta_{c,0}=\rho RT/M_0(1-1/L)\tau_c$, while for the scission-recombination scheme, $\tau_c\sim N^{-1}$ and $\eta_{c,0}=\rho RT/M_0(1-1/L)\vartheta\tau_{c,L}$. Thus, $\eta_{c,0}=\vartheta\eta_{c,0,L}$, with $\vartheta\simeq 1$ for monomer-mediated dynamics, and $\vartheta\simeq 0.83$ for scission-recombination reaction kinetics (the last number depends slightly on L).

Figure 1 presents logarithmic plots for the real and imaginary parts of the complex viscosity as a functions of the dimensionless frequency $\omega_R=\tau_0\omega\equiv(8/\pi^2)\omega_r$ for three polydisperse systems characterized by the same average chain lengths L but different chemical dynamics. The plots

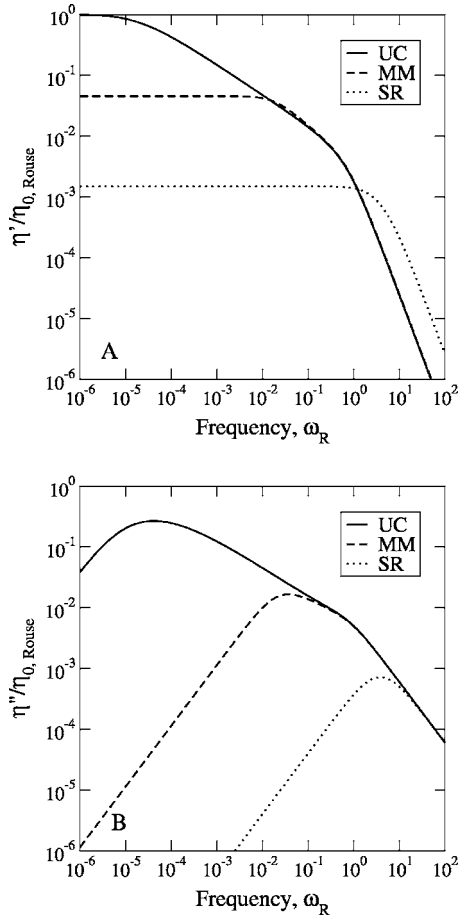

FIG. 1. Normalized dynamic viscosities for three equilibrium polymerizing systems with identical average chain lengths $L=100$ as a function of the dimensionless frequency $\omega_R=\tau_0\omega$. The curves correspond to unbreakable chains (UCs) and to living polymers with monomer-mediated (MM) mass exchanges and with scission-recombination (SR) reaction kinetics. For two last cases, $\tau_0k_D=0.01$. Real components of the shear viscosity η' are displayed in part (A), while imaginary components η'' are presented in part (B).

are normalized by the zero-frequency shear viscosity for unbreakable chains with the same polydispersity. The three curves correspond to (a) frozen chains, i.e., $\lambda_N=0$, (b) monomer-mediated reaction kinetics with $\lambda_N=\pi^2\tau_0k_D/4$, and (c) the scission-recombination mechanism with $\lambda_N=\pi^2\tau_0k_D(2L+N)/8$. Identical dissociation rate constants "per site" k_D and structural relaxation times τ_R are used for the two reacting systems. Chemical relaxation leads to faster stress relaxation, diminishes the viscoelasticity for lower frequencies, and shifts the peak in the imaginary part to higher frequencies. The "tail" of the imaginary part of the viscoelastic function for high frequencies $\tau_0\omega\gg 1$ is unaffected by the chemical dynamics as demonstrated in Fig. 1(b) and as also deduced by analysis of Eq. (27). However, in general, cases (b) and (c) exhibit a quite different ω dependence to the complex viscosity. For monomer-mediated polymerization, the zero-shear viscosity is higher, while the real part of $\eta^*(\omega)$ depends more strongly on frequency than for the scission-recombination mechanism, provided the kinetic rate constants per site are the same. However, if both kinetic rate constants k_A and k_D are scaled to make the zero-frequency shear viscosities for cases (b) and (c) coincide, the whole ω curves become superimposed, with the relative difference not

exceeding 10%. In order to achieve this superposition, the rate constants in Fig. 1 have to be scaled down for the scission-recombination model, or, equivalently, they are both scaled up for monomer-mediated kinetics by a factor of ~190. These results imply that it is difficult to distinguish between these two mechanisms only from an analysis of the frequency dependence of the viscoelastic function without independent information on the reaction rates.

The complex dielectric permittivity for Rouse model chains may be found in a similar fashion. However, the contour integration used for evaluating the finite discrete sum for the Fourier-Laplace transform of the normalized decay function could not completely be resolved analytically, and two additional integrals NJ_N and NJ'_N remain to be calculated numerically. When N is sufficiently large, these integrals yield small corrections since both scale as N^{-1}. Here the expressions for J_N and J'_N with even N are presented, while the Appendix provides the case of odd N. The complex permittivity is evaluated from averaging over the mass distribution

$$\varepsilon^*_{c,N}(\omega) - \varepsilon_{\infty,N} = \Delta\varepsilon \Omega^*_N(\omega), \tag{31}$$

where the reduced frequency dependent part for even N is

$$\Omega^*_N(\hat{\omega}_r) = \frac{\hat{\lambda}_N}{\hat{\lambda}_N + i\hat{\omega}_r} + i\hat{\omega}_r \left[\frac{\tanh(N \operatorname{arcsinh} \sqrt{\hat{\lambda}_N + i\hat{\omega}_r})}{N\sqrt{\hat{\lambda}_N + i\hat{\omega}_r}\sqrt{1+\hat{\lambda}_N + i\hat{\omega}_r} \operatorname{arcsinh}^2 \sqrt{\hat{\lambda}_N + i\hat{\omega}_r}} + \frac{8N}{\pi^2} J'_N \right] - \frac{8N}{\pi^2} J_N, \tag{32}$$

where $\hat{\lambda}_N = 2\lambda_N$, and $\hat{\omega}_r = 2\omega_r$. The coefficient of 2 arises from the difference in the structural relaxation times τ_p in expressions for viscoelastic and dielectric functions of the same factor.

The real and imaginary components yield the contributions to the dynamic dielectric constant and dielectric loss, $\Omega^*_N(\omega_r) = \Omega'_N - i\Omega''_N$,

$$\Omega'_N(\hat{\omega}_r) = \frac{\hat{\lambda}_N^2}{\hat{\lambda}_N^2 + \hat{\omega}_r^2} + \frac{i\hat{\omega}_r}{2}\{f_\varepsilon(\hat{z}^+) - f_\varepsilon(\hat{z}^-)\} - \frac{8N}{\pi^2} J_N, \tag{33}$$

$$\Omega''_N(\hat{\omega}_r) = \frac{\hat{\lambda}_N \hat{\omega}_r}{\hat{\lambda}_N^2 + \hat{\omega}_r^2} - \frac{\hat{\omega}_r}{2}\{f_\varepsilon(\hat{z}^+) + f_\varepsilon(\hat{z}^-)\} - \frac{8N\hat{\omega}_r}{\pi^2} J'_N, \tag{34}$$

where $\hat{z}^\pm = \hat{\lambda}_N + i\hat{\omega}_r$, the functions $f_\varepsilon(\hat{z}^\pm)$ have the same structure as the first term in square brackets in Eq. (32),

$$f_\varepsilon(\hat{z}^\pm) = \frac{\tanh(N \operatorname{arcsinh} \sqrt{\hat{z}^\pm})}{N\sqrt{\hat{z}^\pm}\sqrt{1+\hat{z}^\pm} \operatorname{arcsinh}^2 \sqrt{\hat{z}^\pm}}, \tag{35}$$

and the ω- and N-dependent correction terms J_N and J'_N are obtained as the integrals (N even),

$$J_N = \int_0^\infty \frac{x \tanh(\pi x/2)}{(x^2+N^2)^2} \frac{f_N^2(x)dx}{f_N^2(x) + \hat{\omega}_r^2}, \tag{36}$$

$$J'_N = \int_0^\infty \frac{x \tanh(\pi x/2)}{(x^2+N^2)^2} \frac{f_N(x)dx}{f_N^2(x) + \hat{\omega}_r^2}, \tag{37}$$

with $f_N(x) = \cosh^2(\pi x/2N) + \hat{\lambda}_N$. Equations for unbreakable chains, i.e., with infinite lifetimes, are generated by setting $\hat{\lambda}_N = 0$ and averaging over the mass distribution. Naturally, the first term in Eq. (32) vanishes in that case.

The frequency dependent dielectric permittivity exhibits similar trends as for the viscoelastic properties. As is seen from the normalized dielectric loss spectrum $E'' = \varepsilon''/\Delta\varepsilon$ (see Fig. 2), more "rapid" chemical dynamics produces a narrower peak, and the maximum shifts towards higher frequencies because of the smaller effective stress relaxation time. When the chains are sufficiently long, the corrections J_N and J'_N become negligible, and the closed form analytical formula for dielectric relaxation is reliable. The "worst" approximation in neglecting J_N and J'_N is for the model with $\hat{\lambda}_N = 0$ (unbreakable chains). Figure 3 presents the ratios of absolute values of the complex dielectric permittivity for different frequencies and chain lengths in the Rouse model as evaluated using Eq. (32) with the correction terms J_N and J'_N neglected and as calculated without this approximation by performing the direct summation over all the modes [see Appendix, Eq. (A8)]. The relative error increases with frequency. However, within the frequency range of $0 \leqslant \omega_R \leqslant 0.1$, the absolute

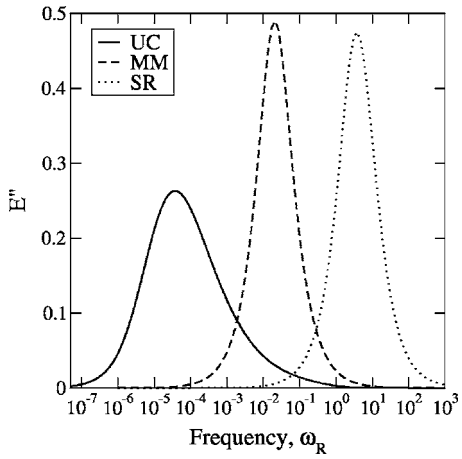

FIG. 2. Normalized dielectric loss E'' as a function of dimensionless frequency ω_R for three systems with equal average chain lengths $L=100$ and different relaxation dynamics. The three systems are unbreakable chains (UCs) and living polymers follow the monomer-mediated (MM) and scission-recombination (SR) reaction kinetics. For living polymers, $\tau_0 k_D = 0.01$.

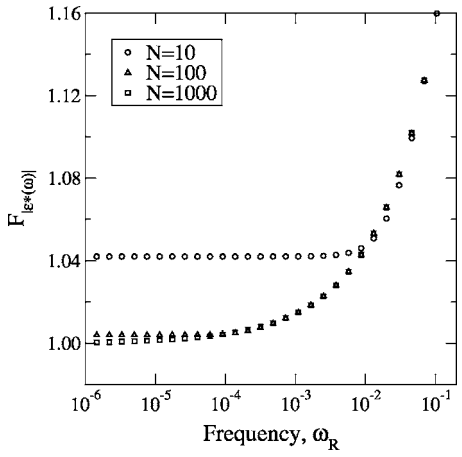

FIG. 3. The ratio of absolute values of the dielectric permittivity in the Rouse model as evaluated using Eq. (32) neglecting the correction terms J_N and J'_N and as calculated by direct summation over the normal modes as function of dimensionless frequency ω_R for different chain lengths.

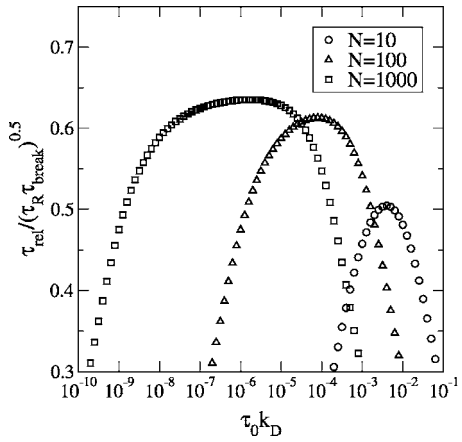

FIG. 4. Comparison between the effective stress relaxation times for polymer systems following Rouse dynamics evaluated using the present theory and the model of Cates and co-workers for various values of the parameter $\tau_0 k_D$ and the chain lengths N (see text). The chemical reaction dynamics is assumed to proceed through the reversible scission-recombination (SR) model mechanism. The middle "plateau" regime delineates the range of kinetic parameters over which there is general agreement between both theories, while the departure from this plateau for large $\tau_0 k_D$ demonstrates the difference between the models in the $\xi \ll 1$ regime. The departure from the plateau level for small $\tau_0 k_D$ arises because the square root coupling expression of Eq. (42) in the model of Cates and co-workers is not applicable when $\xi > 1$.

value of the dielectric permittivity changes by approximately two orders of magnitude for chains of length $N=100$ and approximately three orders of magnitude for chains with $N=1000$, while the relative overestimation of $|\varepsilon^*(\omega_R)|$ is at most only 1.16.

IV. SELECTED APPLICATIONS

A. Brief comparison to model by Cates and co-workers

The model by Cates and co-workers focuses on the particular dynamic regime in which the average time $\tau_{break} \simeq 1/(k_D N)$ for a chain of length N to break into two pieces is lower than the characteristic time of stress relaxation τ_{rel} for unbreakable "representative" chains of the same length. The characteristic stress relaxation time τ is generally affected by the scission-recombination reaction kinetics within the model of Cates and co-workers, and τ is identified with the waiting time for a break in the chain to occur within some characteristic arc distance n.[29] The contour distance n, which is usefully "utilized" for the stress relaxation, is estimated from scaling arguments. These arguments assume that the relaxation time τ_{rel} for a section of chain n (say, the Rouse time $\tau_0 n^2$ when Rouse-type dynamics are considered) is comparable to τ_{break}. The overall relaxation time τ in the regime $\tau_{break} \ll \tau_{rel}$ is then given by

$$\tau \simeq \tau_{break} N l^2 / \langle r^2(\tau_{break}) \rangle, \tag{38}$$

where $\langle r^2(\tau_{break}) \rangle$ is the mean-square displacement of a monomer on an unbreakable chain of length N in a time τ_{break} (l is a subunit length).

In order to compare some predictions between our model and that of Cates and co-workers, attention is restricted to the scission-recombination polymerization mechanism in conjunction with the Rouse model described above, and it suffices to compare predictions for contributions from chains of length N. The zero frequency shear viscosity within our theory immediately follows from Eq. (22) as

$$\eta_{0,N} = \frac{\rho N_A \zeta_0 b^2}{24 M_0} \left[\frac{\coth(2N \operatorname{arcsinh} \sqrt{\lambda_N})}{\sqrt{\lambda_N}\sqrt{1+\lambda_N}} - \frac{1}{2N}\left(\frac{1}{\lambda_N} + \frac{1}{1+\lambda_N}\right)\right] \equiv G_{0,N}\tau, \tag{39}$$

where $G_{0,N} = G'_{max,N}(\omega) = \rho RT(1-N^{-1})/M_0$ is the plateau modulus,

$$\tau = \frac{\pi^2}{8}\left(\frac{\tau_0}{N-1}\right)\left[\frac{\coth(2N \operatorname{arcsinh} \sqrt{\lambda_N})}{\sqrt{\lambda_N}\sqrt{1+\lambda_N}} - \frac{1}{2N}\left(\frac{1}{\lambda_N} + \frac{1}{1+\lambda_N}\right)\right], \tag{40}$$

$\tau_0 = \zeta_0 b^2/3\pi^2 k_B T$ is the "Rouse constant," and

$$\lambda_N = \frac{\pi^2 \tau_0 k_D (2L+N)}{8}. \tag{41}$$

Note that if $\tau_c \to 0$, the stress relaxation is exponential with time constant $\tau \to \tau_c$, and the average zero-shear viscosity $\eta_{c,0}$ is given by Eq. (30).

The model of Cates and co-workers predicts that if the chain motion is also Rouse-type and if $\tau_{break} \ll \tau_R$, the viscosity obeys the scaling relation,[6]

$$\eta_{0,N} \simeq G_{0,N}(\tau_R \tau_{break})^{1/2} = \gamma G_{0,N}(N\tau_0/k_D)^{1/2}, \tag{42}$$

where $\tau_R \simeq \tau_0 N^2$ is the Rouse time of an unbreakable chain of length N, $G_{0,N}$ is the plateau modulus, γ is a constant of the order of unity which cannot be calculated exactly, and τ_0 is defined above. Equations (39)–(42) imply that the zero frequency shear viscosity in both the model of Cates and coworkers and our model can be represented as a function of

the universal dimensionless parameter $\tau_0 k_D$ since Eq. (42) can be rewritten as $\eta_{0,N}=\gamma G_{0,N}\tau_0(N/\tau_0 k_D)^{1/2}$.

The direct comparison between two approaches may be effected for $\eta_{0,N}/G_{0,N}\tau_0$ at fixed ρ, τ_0, T by varying both k_D and k_A in parallel while maintaining as constant the mean length $L\simeq N$. Figure 4 compares the two approaches for the dependence of the ratio of values for $\eta_{0,N}/G_{0,N}\tau_0$ from two models on the kinetic rate constants. Each curve corresponds to chains of fixed length N. A range of dissociation rate constants exists in which the two theories agree qualitatively apart from a factor of the order of unity. This range becomes larger for longer chains, and the agreement only occurs within the limits in which the model of Cates and co-workers is applicable, i.e., for $\xi=\tau_c/\tau_R\simeq(\tau_0 k_D N^3)^{-1}\leqslant 1$. The ratio between the values of $\eta_{0,N}/G_{0,N}$ for the two models is roughly a constant within some range of $\tau_0 k_D$, being close to 0.5. The difference between the approaches occurs for small k_D (and k_A) where the model of Cates and co-workers is not applicable because his "scaling" model does not reduce to a description of frozen, unbreakable, polydisperse polymers in the limit of vanishing k_D as in our theory and as in the general formulation of Cates and co-workers (see below). A difference between the theories also emerges for very large values of the kinetic rate constants. This is illustrated for $\tau_0 k_D$ varying between 10^{-6} and 10^{-3}, where the effective stress relaxation times in the present model and in the model of Cates and co-workers change in a parallel fashion for "intermediate" sized chains ($N=100$), while the model of Cates and co-workers is inapplicable over most of the range for "short" chains ($\xi>1$). A departure between our model and that of Cates and co-workers is evident for very rapid reaction kinetics ($\xi\ll 1$) of "long" chains. Applying the scaling theory of Cates and co-workers type to Rouse-type dynamics suggests that the coupling $\tau\simeq(\tau_R\tau_{\text{break}})^{1/2}$ is valid in the small $\tau_c\simeq\tau_{\text{break}}$ regime, while our approximation suggests that the asymptotic time constant τ approaches the lifetime τ_c as $\tau_c\to 0$.

Granek and Cates[26] also derive an analytical approximation for the stress relaxation function for living polymers in the framework of a Poisson renewal model. Their expression yields a relation (in Laplace transform space) between the stress relaxation function $\mu_{rm}(t)=G_{rm}(t)/G_{rm,0}$ for living polymers in a chemically reversible system and the stress relaxation function $\mu_N(t)=G_N(t)/G_{0,N}$ for unbreakable chains of length N. Here $G_{rm,0}$ and $G_{0,N}$ are the plateau moduli for living polymer and unbreakable polymers of length N, respectively. The Poisson model relies on the assumption that no correlation exists in the dynamics between renewal intervals and that during one renewal interval. Hence, the stress relaxation is taken as independent of what transpired within the previous interval. The complex viscosity of the polymer system in the renewal model is

$$\eta^*_{rm}(i\omega)=\frac{\int_0^\infty dN N c_N \eta^*_N(i\omega+\tau_c^{-1})}{1-\int_0^\infty dN N c_N \tau_c^{-1} G_{0,N}^{-1}\eta^*_N(i\omega+\tau_c^{-1})}, \tag{43}$$

where $\eta^*_N(s)$ denotes the complex viscosity for a system of unbreakable chains, $\eta^*_N(s)=\int_0^\infty dt e^{-st}G_{0,N}\mu_N(t)$ and the average over the mass distribution is explicitly indicated. Thus, $G_{rm}(t)$ for a living polymer system is obtained from a multiple convolution of $G_c(t)$ from Eq. (9) [see Eq. (43) above]. The transform $G^*_{rm}(\omega)$ emerges from the renewal model as a rational fraction of $G^*_c(\omega)$, so we focus attention on the basic quantities $G_c(t)$ and its transform $G^*_c(\omega)$. Hence, our results may readily be converted into those for the renewal model.

The renewal model is now used to describe viscoelastic properties of a polymer system where a dominant mechanism for the stress relaxation is chain reptation. The stress relaxation function for the reptation model is

$$\begin{aligned}\mu(t)&=\frac{1}{L^2}\int_0^\infty N\exp(-N/L)\mu_N(t)dN\\&=\frac{8}{L^2\pi^2}\sum_{p=1}^{\infty}\frac{1}{p^2}\int_0^\infty N\exp(-N/L)\\&\quad\times\exp(-tp^2/\tau_{\text{rep}})dN\quad(p\text{ odd}),\end{aligned}\tag{44}$$

where $\tau_{\text{rep}}=\bar{\tau}_{\text{rep}}(N/L)^3$ is the reptation time of a chain of length N and $\bar{\tau}_{\text{rep}}$ is that of a chain with the average length L. In the limit of small τ_c, the sum over p can be replaced by an integral. After averaging over the chain length distribution (exponential as usual), the effective stress relaxation time $\tau\sim\eta_c(\omega=0)$ for the living polymers in the SR model with $\tau_c=\tau_{\text{break}}/(2+N/L)$ is given by $\tau=\alpha(\tau_{\text{break}}\bar{\tau}_{\text{rep}})^{1/2}$ with $\alpha\simeq 0.38$.[26] Use of the full expression for $\mu_N(t)$ in Eq. (44) for unbreakable *reptative* chains is essential to obtain this particular square root dependence of τ on the scission time τ_{break}. Note that both our model and the renewal model produce the correct result for infinitely long τ_c. The viscosity for a system of unbreakable chains, with an identical chain length distribution as the living polymer system, is obtained in this limit as expected from our theory.

If the polymer dynamics is Rouse-type and if $\tau_c>\tau_0$, our model and the renewal approximation are in agreement because the time scales in both expressions are combined using the harmonic mean of τ_p and τ_c. However, as τ_c becomes smaller (say, less than τ_0), the difference between the models is evident since the denominator in Eq. (43) is distinct from unity and diminishes as τ_c gets smaller.

Cates suggests that for Rouse dynamics, the assumption of independent stress relaxation in different renewal intervals fails because the low frequency modes are more affected by chain length "jumps" in renewal events than the "local," high frequency modes. We believe that it is still an open question as to what is the proper limit for the stress relaxation when the chemical relaxation is very fast and as to how the effective time τ for this process depends on τ_c. The prediction of our model emerges from Eqs. (30) and (40) in the limit of $\lambda_N^{-1}\to 0$. The Appendix presents a closed form resolution of the transform $\eta_N(\omega)=G_{0,N}\mu_N(\omega)/i\omega$ of Eq. (44) and the transform $\eta_{c,N}(\omega)$, i.e., the viscoelastic function as modified by chemical relaxation processes for the reptation model.

B. On qualitative nature of relaxation in associating fluids

When the chain lifetime is very large for unbreakable reptative chains, i.e., $\tau_c\to\infty$, the stress relaxation for mono-

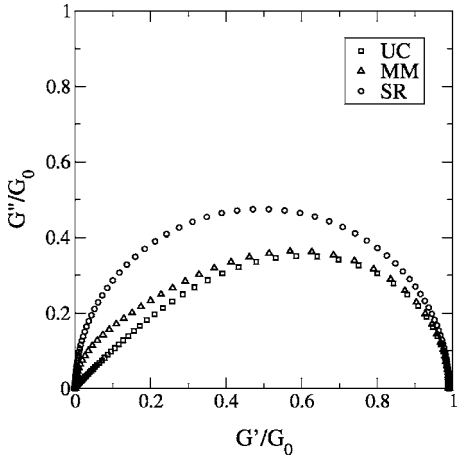

FIG. 5. Cole-Cole plots for Rouse model polymer systems with $L=100$ and with different reversible dynamics: unbreakable chains (UCs), monomer-mediated polymerization (MM), and scission-recombination (SR) reaction kinetics. For both systems of living polymer chains (MM and SR), the parameter $\tau_0 k_D$ is equal to 0.01.

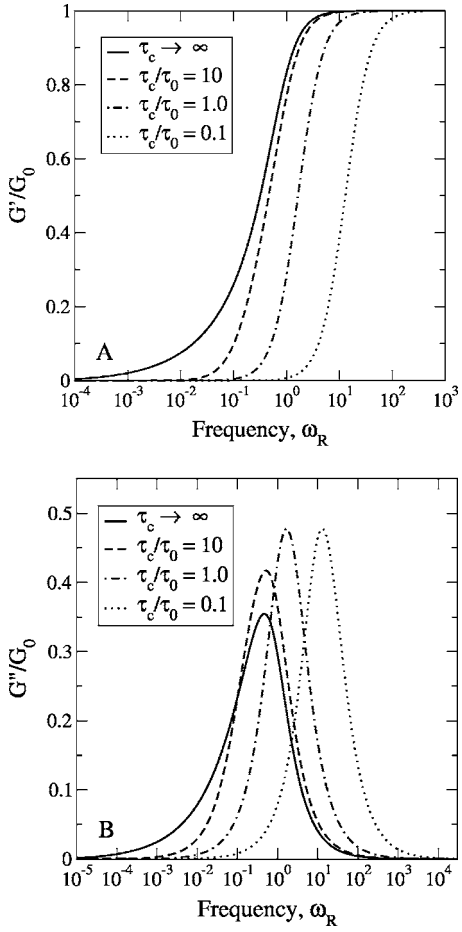

FIG. 6. The normalized complex modulus G^* as function of dimensionless frequency $\omega_R=\tau_0\omega$ for equilibrium polydisperse systems with scission-recombination (SR) model reaction kinetics and average chain length $L=100$. Real components G' are displayed in part (A) while imaginary components G'' are presented in part (B). The parameters τ_c/τ_0 are in legends, where τ_c is the mean lifetime of an average chain of length L and τ_0 is the Rouse constant (see text). The solid curves correspond to unbreakable chains with $\tau_c \to \infty$.

disperse systems is nonexponential, as found for the Rouse model. On the other hand, averaging over the exponential equilibrium distribution in Eq. (5) in the limit of very slow, nearly frozen chemical dynamics does not produce qualitatively new features in the time dependence of $G(t)$. A stretched exponential approximation $G(t) \sim e^{-at^\beta}$ fits $G(t)$ over a limited range of times. The calculated β is altered if the sum over p in Eq. (5) is truncated to retain only the slowest $p=1$ mode (a description that has been used as a crude model of stress relaxation in glass forming liquids).[30] The stress relaxation becomes exponential at very large times t. The lifetime for the long time exponential decay of monodisperse systems is proportional to N^2, as expected. When the chemical dynamics becomes faster, the relaxation spectrum for a polydisperse system changes from rather disperse to nearly exponential for all times.

The evolution of the stress relaxation spectrum as the rate of assembly-disassembly kinetics switches from being slow to fast may be followed in the frequency domain as well. The analysis of this frequency dependence is conveniently represented in terms of Cole-Cole plots, in which, for instance, the imaginary part of the complex modulus $G''(\omega)$ is presented as a function of the real part $G'(\omega)$, or analogously, the imaginary component of the dielectric permittivity $\varepsilon''(\omega)$ is plotted versus the real component $\varepsilon'(\omega)$ in order to analyze the dynamics of viscoelastic and dielectric relaxation, respectively.[31,32] Systems with a single exponential decay yield perfectly semicircular Cole-Cole plots, characteristic of those for a Maxwell model. In general, deviations from semicircular plots appear and are indicative of nonexponential stress relaxation.

Figure 5 presents a redrawing of the data from Fig. 1 in form of Cole-Cole plots for the normalized complex modulus $G^*(\omega)/G_0$ of a set of Rouse model polymer systems with different reaction kinetics but with identical equilibrium macromolecular distributions. Frozen Rouse chains [unbreakable chains (UC)] yield a nonsymmetric Cole-Cole plot, while the plots become close to semicircular for scission-recombination model living chains (SR) that can break and recombine freely. The plot for MM reaction kinetics lies intermediate. However, for sufficiently rapid chemical dynamics (large values of k_D and k_A), the Cole-Cole plot again approaches a semicircle. Thus, based on an analysis of the shape of the Cole-Cole plot for a reversibly aggregating system, the relaxation spectrum may be deduced as either nearly exponential, which is characteristic of that for a living polymer system with an effective interplay between the kinetic mechanism of viscoelastic relaxation and stress relaxation due to chain motions, or as quite disperse, indicative of "unbreakable" macromolecules with negligible mass redistribution.

To demonstrate the general trends, Fig. 6 presents the frequency dependence of the real and imaginary components of the normalized complex modulus $G'(\omega)/G_0$ and $G''(\omega)/G_0$ for polydisperse system following scission-recombination dynamics for systems with average chain length $L=100$. The relaxation spectrum shifts to higher frequencies as the characteristic times for the scission-recombination reaction τ_c decrease and the chemical relax-

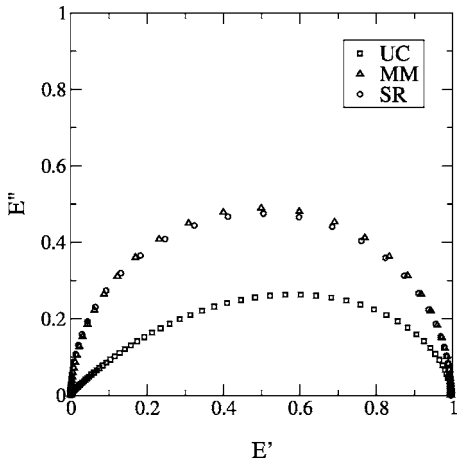

FIG. 7. The dependence of the imaginary component of the normalized dielectric permittivity E'' on its real part E' for equilibrium polymerization systems with $L=100$: unbreakable chains (UCs) and living polymers with monomer-mediated (MM) and scission-recombination (SR) kinetics. The living chains are described using $\tau_0 k_D=0.01$.

ation becomes faster. It is interesting to contrast the Cole-Cole plot for unbreakable chains, whose dominant stress relaxation mechanism is reptation, with those whose relaxation follows a Rouse model. The high frequency part of the Cole-Cole plot for a purely reptative mechanism passes through the point (1,0) with an asymptotic of slope -1,[31] while this part of the plot for Rouse-type dynamics is close to a semicircular shape.

Cole-Cole plots for the normalized dielectric permittivity are presented in Fig. 7 for the three different reaction models. The characteristic times τ_c for the chemical reactions (1) and (2) in the Cole-Cole plots in Figs. 5 and 7 lie within the range of structural relaxation times τ_p for the representative chains with $N=100$. Indeed, for monomer-mediated kinetics, $\tau_c/\tau_p \simeq p^2/(k_D\tau_0 N^2) \simeq 1$ for $p \simeq 10$ since $k_D\tau_0=0.01$ in the figures, while the characteristic time for scission-recombination reaction is comparable with the "shortest" structural relaxation time τ_0 since $\tau_c/\tau_0 \simeq 1/(k_D\tau_0 N) \simeq 1$. The choice of parameters ($\tau_0 k_D$ and L) leads to Cole-Cole plots for the dielectric relaxation of living polymer systems with both SR and MM reaction schemes that are symmetric and close to semicircular, while only the system with scission-recombination dynamics exhibits a semicircular viscoelastic Cole-Cole diagram. However, as noted above, parameters can be chosen to superimpose the viscoelastic (as well as the two dielectric) functions for scission-recombination and monomer-mediated kinetics. This identity is achieved for monodisperse system using $k_{D,\mathrm{SR}} \simeq k_{D,\mathrm{MM}}/N$.

V. CONCLUSIONS

The influence of reversible chemical dynamics in linear macromolecules on their viscoelastic functions and dielectric relaxation is studied by analyzing two different reaction mechanisms that correspond to monomer-mediated (MM) model and scission-recombination (SR) model polymerizations. Analytical expressions for the complex viscosity and the dielectric permittivity for Rouse chains are derived in closed form within the bead-spring model for chains of fixed length N. The general analysis for extremely slow chemical relaxation in equilibrium reversibly aggregating systems demonstrates that the only influence on the dynamic properties of the system is associated with the polydisperse macromolecular distribution, and the viscoelastic and dielectric functions correspond in that limit to those for a polydisperse system of "unbreakable" chains. When the chain scission times are comparable to times within spectrum of the structural relaxation times or when the chemical dynamics is rapid on the time scales of internal chain motions, the interplay between the chemical reaction events and the structural rearrangements increases the stress relaxation rate, often considerably, and the relaxation effectively becomes a single exponential decay.

The present approach is compared with that of Cates and co-workers for Rouse dynamics using a different model for the coupling between the kinetic and "regular" (e.g., Rouse-type or reptative) mechanisms. Within the domain of applicability of the approximations of Cates and co-workers, both models produce similar results for quite long chains. However, the predictions of the models are different for very rapid chemical dynamics where experimental data are unavaiable and numerical simulation results are lacking.

By proper choice of the chemical reaction rate constants for both reaction mechanisms, the respective viscoelastic and dielectric functions can be brought into nearly full coincidence over the whole range of frequencies for equilibrium aggregating system that follows monomer-mediated and scission-recombination kinetics.

A closed form expression is obtained for the contributions from chains of length N to the viscoelasticity of reptating polymers that are affected by the reaction kinetics. An analysis of the expression derived for the viscoelasticity indicates that for infinitely long τ_c, the theory recovers the viscoelastic function of unbreakable reptative chains as required, while when the chain scission times are finite, the stress relaxation is influenced by an interplay of single chain dynamics and chemical relaxation.

ACKNOWLEDGMENTS

This research is supported, in part, by NSF Grant No. CHE-0416017 and PRF Grant No. 41728-AC7. The authors thank J. F. Douglas for valuable discussions.

APPENDIX: EVALUATION OF FINITE TRIGONOMETRIC SERIES BY CONTOUR INTEGRATION

1. The bead-spring model with reversible chemical dynamics: Viscoelastic function

The calculation of dynamic properties, such as viscosity and dielectric permittivity in our model requires the evalua

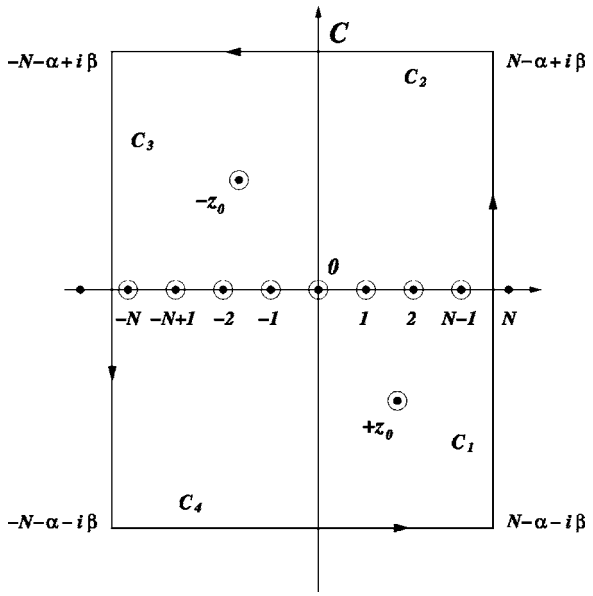

FIG. 8. Integration contour used for analytically evaluating the finite series for the viscoelastic function in the Rouse model. Here α is an arbitrary positive constant less than unity and β is taken to approach infinity. The circled points are simple poles of the auxiliary contour function (see text).

tion of finite series involving trigonometric functions. We use contour integration to resolve these series into closed form.[33,34]

Consider the contour C in the complex plane z as shown in Fig. 8 where α is an arbitrary constant between 0 and 1 while β is taken to approach infinity. Next, we exactly evaluate the finite sum necessary for calculating the contribution $\eta^*_{c,N}(\omega)$ from chains of length N to the complex viscosity,

$$\eta^*_{c,N}(\omega) = \frac{\rho RT}{M}\sum_{p=1}^{N-1}\frac{1}{\kappa^{-1}\sin^2(\pi p/2N)+\tau_c^{-1}+i\omega} = \frac{\kappa\rho RT}{M}\sum_{p=1}^{N-1}\frac{1}{\sin^2(\pi p/2N)+\lambda_N+i\omega_r} = \frac{\rho N_A\zeta_0 b^2}{24M}S_N, \tag{A1}$$

with the prefactor κ defined above Eq. (23). To evaluate S_N, consider the contour integral

$$I_N = \oint_C \frac{\cot(\pi z)dz}{\sin^2(\pi z/2N)+\lambda_N+i\omega_r} = \oint_C F_N(z)dz, \tag{A2}$$

with C of Fig. 8. The integrations along the horizontal portions C_2 and C_4 vanish as $\beta\to+\infty$ since $\sin(\pi z/2N)\to+\infty$ for $|z|\to+\infty$. After noting that $\cot(z)$ and $\sin^2(z)$ both have a period of π, it is seen that integrands for the integrals along C_1 and C_3 are both equal to $\cot(\pi\xi)/(\sin^2(\pi\xi/2N)+\lambda_N+i\omega_r)$ ($\xi=\alpha+i\beta$, β varies), but they are traversed in opposite directions. Hence, these two integrals compensate each other, and the integral I_N vanishes,

$$\oint_C \frac{\cot(\pi z)}{\sin^2(\pi z/2N)+\lambda_N+i\omega_r} = 0. \tag{A3}$$

On the other hand, $F_N(z)$ (for $N\geqslant 2$) has simple poles at $z=0,\pm1,\pm2,\ldots,\pm(N-1),-N$ and $z=\pm z_0$ with $z_0=(2Ni/\pi)\operatorname{arcsinh}\sqrt{\lambda_N+i\omega_r}$, all lying within the contour C. Application of the residual theorem to Eq. (A3) yields after rearrangement,

$$\sum_{p=1}^{N-1}\operatorname{Res}\{F(z),z=\pm p\}+\operatorname{Res}\{F(z),z=-N\} + \operatorname{Res}\{F(z),z=0\}+\operatorname{Res}\{F(z),z=\pm z_0\}=0. \tag{A4}$$

For $p=0,\pm1,\ldots,\pm N$, the residues are evaluated as

$$\operatorname{Res}\{F(z),z=\pm p\} = \frac{1}{\pi(\sin^2(\pi p/2N)+\lambda_N+i\omega_r)}, \tag{A5}$$

while

$$\operatorname{Res}\{F(z),z=\pm z_0\} = -\frac{N\coth(2N\operatorname{arcsinh}\sqrt{\lambda_N+i\omega_r})}{\pi\sqrt{\lambda_N+i\omega_r}\sqrt{1+\lambda_N+i\omega_r}}. \tag{A6}$$

Hence, after substitution into Eq. (A4), we have the exact result

$$(2/\pi)S_N+\frac{1}{\pi(\lambda_N+i\omega_r)}+\frac{1}{\pi(1+\lambda_N+i\omega_r)} - \frac{2N\coth(2N\operatorname{arcsinh}\sqrt{\lambda_N+i\omega_r})}{\pi\sqrt{\lambda_N+i\omega_r}\sqrt{1+\lambda_N+i\omega_r}}=0. \tag{A7}$$

Substituting S_N into Eq. (A1) and using the relation $M=NM_0$ produce Eq. (22). The separation of complex viscosity into the real and imaginary components may be checked by direct substitution, but they may be evaluated separately by contour integration beginning from the expressions for $\eta'_{c,N}$ and $\eta''_{c,N}$ in the form of separate series.

2. The bead-spring model with reversible chemical dynamics: Dielectric relaxation

The average over internal chain modes for the dielectric permittivity constant as a function of frequency can be derived similarly. However, contour integration does not produce a closed form since the integral of the auxiliary function over the contour is distinct from zero and is not known in closed form. In spite of this, a quite good closed form approximation can be derived. Consider the case of even N first. Define the integration contour in the same way as in Fig. 8 but with $\alpha=0$. We need to calculate

$$\Omega^*_N(\omega) = \frac{\varepsilon^*_{c,N}(\omega)-\varepsilon_{\infty,N}}{\Delta\varepsilon} = \frac{8}{\pi^2}\sum_{p=1}^{N-1}\frac{1}{p^2}\frac{(1/2)\kappa^{-1}\sin^2(\pi p/2N)+\tau_c^{-1}}{(1/2)\kappa^{-1}\sin^2(\pi p/2N)+\tau_c^{-1}+i\omega} = \frac{8}{\pi^2}\sum_{p=1}^{N-1}\frac{1}{p^2}\frac{\sin^2(\pi p/2N)+\hat{\lambda}_N}{\sin^2(\pi p/2N)+\hat{\lambda}_N+i\hat{\omega}_r} = \frac{8}{\pi^2}S'_N \tag{A8}$$

by summing over odd p. Here $\hat{\lambda}_N=2\lambda_N$, and $\hat{\omega}_r=2\omega_r$ following from the definition of Eqs. (9) and (13). To evaluate S'_N, apply the contour integral

$$I'_N=\oint_{C'}\frac{\tan(\pi z/2)dz}{z^2}\frac{\sin^2(\pi z/2N)+\hat{\lambda}_N}{\sin^2(\pi z/2N)+\hat{\lambda}_N+i\hat{\omega}_r}$$
$$=\oint_{C'}F'_N(z)dz, \tag{A9}$$

with C' of Fig. 8 and with $\alpha=0$. The integrations along horizontal parts C'_2 and C'_4 vanish as $|\beta|\to+\infty$ since $|z^2|\to+\infty$. The integrals along vertical lines C'_1 and C'_3 are equal to each other. To show this, recall that $\tan(z)$ and $\sin^2(z)$ both have a period of π. Hence, the integrands for the integrals along C'_1 and C'_3 have the integration variables $z_{1,3}=\pm N+i\beta$, (N is an even number, β is a variable) and are given by

$$F'_N(z_{1,3})=\frac{\tan(\pi z_{1,3}/2)}{z_{1,3}^2}\frac{\sin^2(\pi z_{1,3}/2N)+\hat{\lambda}_N}{\sin^2(\pi z_{1,3}/2N)+\hat{\lambda}_N+i\hat{\omega}_r}$$
$$=\frac{i\tanh(\pi\beta/2)}{(i\beta\pm N)^2}\frac{\cosh^2(\pi\beta/2N)+\hat{\lambda}_N}{\cosh^2(\pi\beta/2N)+\hat{\lambda}_N+i\hat{\omega}_r}, \tag{A10}$$

where the plus sign before N applies for $F'_N(z_1)$, while the minus sign is for $F'_N(z_3)$. After simple transformations, we find

$$F'_N(z_1)=\{N^2-\beta^2-2i\beta N\}i\Sigma'_N(\beta),$$
$$F'_N(z_3)=\{N^2-\beta^2+2i\beta N\}i\Sigma'_N(\beta), \tag{A11}$$

where

$$\Sigma'_N(\beta)=\frac{\tanh(\pi\beta/2)}{(N^2+\beta^2)^2}\frac{f_N^2(\beta)-if_N(\beta)\hat{\omega}_r}{f_N^2(\beta)+\hat{\omega}_r^2}, \tag{A12}$$

with $f_N(\beta)=\cosh^2(\pi\beta/2N)+\hat{\lambda}_N$. Recall that in the course of integration the contour parts C'_1 and C'_3 are traversed in opposite directions. Because both parts contribute equally to the contour integral, it becomes

$$I'_N=\oint_{C'}F'_N dz=4iN\int_{-\infty}^{+\infty}\beta\Sigma'_N(\beta)d\beta, \tag{A13}$$

where $dz_{1,3}=id\beta$.

On the other hand, $F'_N(z)(N\geqslant 2)$ has simple poles at $z=0,\pm1,\pm3,\ldots,\pm(N-1)$ (odd numbers) and $z'=\pm z'_0$ with $z'_0=(2Ni/\pi)\operatorname{arcsinh}\sqrt{\hat{\lambda}_N+i\hat{\omega}_r}$ all lying within the contour C'. Application of the residual theorem to Eq. (A13) yields after rearrangement,

$$\sum_{p=1}^{N}\operatorname{Res}\{F'_N(z),z=\pm p:\text{odd}\}+\operatorname{Res}\{F'_N(z),z=0\}+\operatorname{Res}\{F'_N(z),z=\pm z'_0\}$$
$$=\frac{1}{2\pi i}\oint_{C'}F'_N(z)dz. \tag{A14}$$

The residues for $p=\pm1,\ldots,\pm N$ are

$$\operatorname{Res}\{F'_N(z),z=\pm p:\text{odd}\}=-\frac{2}{\pi}\frac{\sin^2(\pi p/2N)+\hat{\lambda}_N}{p^2(\sin^2(\pi p/2N)+\hat{\lambda}_N+i\hat{\omega}_r)}, \tag{A15}$$

for $p=0$ the residue is

$$\operatorname{Res}\{F'_N(z),z=0\}=\frac{\pi\hat{\lambda}_N}{2(\hat{\lambda}_N+i\hat{\omega}_r)}, \tag{A16}$$

while

$$\operatorname{Res}\{F'_N(z),z=\pm z'_0\}=\frac{i\pi\hat{\omega}_r\tanh(2N\operatorname{arcsinh}\sqrt{\hat{\lambda}_N+i\hat{\omega}_r})}{4N\sqrt{\hat{\lambda}_N+i\hat{\omega}_r}\sqrt{1+\hat{\lambda}_N+i\hat{\omega}_r}\operatorname{arcsinh}^2\sqrt{\hat{\lambda}_N+i\hat{\omega}_r}}. \tag{A17}$$

After substituting into Eq. (A14), we have

$$-(4/\pi)S'_N+\frac{\pi\hat{\lambda}_N}{2(\hat{\lambda}_N+i\hat{\omega}_r)}+\frac{i\pi\hat{\omega}_r\tanh(2N\operatorname{arcsinh}\sqrt{\hat{\lambda}_N+i\hat{\omega}_r})}{2N\sqrt{\hat{\lambda}_N+i\hat{\omega}_r}\sqrt{1+\hat{\lambda}_N+i\hat{\omega}_r}\operatorname{arcsinh}^2\sqrt{\hat{\lambda}_N+i\hat{\omega}_r}}=\frac{2N}{\pi}\int_{-\infty}^{+\infty}\beta\Sigma'_N(\beta)d\beta. \tag{A18}$$

Inserting S'_N into Eq. (A8) and redefining the interal I'_N in terms of the pair of integrals J_N, J'_N for real and complex components, Eq. (32) is obtained. Note, that due to symmetry, the integral I'_N is transformed to the limits from 0 to $+\infty$ for J_N, and J'_N, so a coefficient of 2 appears in the final formulas.

Now consider the case of odd N. The vertical lines of the new integration contour C'' are to be shifted parallel to the corresponding lines of contour C' for even N by one unit towards the center [recall the auxillary function $F'_N(z)$ has poles at odd N]. Analogously, the integration along horizontal parts vanishes, while integration along $N-1+i\beta$ and $-N+1+i\beta$ again results in equal contributions (as numerical analysis verifies). The sum of these contributions equals the contour integral I''_N and is given by twice the integral along C''_1. After some algebra, we obtain

$$I''_N=2\oint_{C''}F'_{N-1}dz=-2\int_{-\infty}^{+\infty}\{(N-1)^2-\beta^2-2i(N-1)\beta\}\Sigma''_N(\beta)d\beta=-2J''_N, \tag{A19}$$

with

$$\Sigma_N''(\beta)=\frac{\tanh(\pi\beta/2)}{\{(N-1)^2+\beta^2\}^2}\frac{(x+\hat{\lambda}_N)^2+y(y+\hat{\omega}_r)-i\hat{\omega}_r(x+\hat{\lambda}_N)}{(x+\hat{\lambda}_N)^2+(y+\hat{\omega}_r)^2}, \tag{A20}$$

where $x=1/2[1+\cos(\pi/N)\cosh(\pi\beta/N)]$ and $y=1/2\sin(\pi/N)\sinh(\pi\beta/N)$. Analogous to Eq. (A14) for odd N, I_N'' is

$$-(4/\pi)S_N'+\frac{\pi\hat{\lambda}_N}{2(\hat{\lambda}_N+i\hat{\omega}_r)}+\frac{i\pi\hat{\omega}_r\tanh(2N\,\mathrm{arcsinh}\,\sqrt{\hat{\lambda}_N+i\hat{\omega}_r})}{2N\sqrt{\hat{\lambda}_N+i\hat{\omega}_r}\sqrt{1+\hat{\lambda}_N+i\hat{\omega}_r}\,\mathrm{arcsinh}^2\,\sqrt{\hat{\lambda}_N+i\hat{\omega}_r}}=\frac{1}{2\pi i}I_N'', \tag{A21}$$

and hence

$$\Omega_N^*(\hat{\omega}_r)=\frac{\hat{\lambda}_N}{\hat{\lambda}_N+i\hat{\omega}_r}+\frac{i\hat{\omega}_r\tanh(2N\,\mathrm{arcsinh}\,\sqrt{\hat{\lambda}_N+i\hat{\omega}_r})}{N\sqrt{\hat{\lambda}_N+i\hat{\omega}_r}\sqrt{1+\hat{\lambda}_N+i\hat{\omega}_r}\,\mathrm{arcsinh}^2\,\sqrt{\hat{\lambda}_N+i\hat{\omega}_r}}-\frac{2i}{\pi^2}J_N'', \tag{A22}$$

where J_N'' is presented in Eqs. (A19) and (A20).

3. Reptation model: Viscoelastic functions

The contribution to the complex viscosity from chains of fixed length N for the reptation model are affected by chemical relaxation,

$$\eta_{c,N}^*(\omega)=\frac{8}{\pi^2}G_{0,N}\sum_{p=1}^{\infty}\frac{1}{p^2(p^2\tau_{\mathrm{rep}}^{-1}+\tau_c^{-1}+i\omega)}=\frac{8}{\pi^2}G_{0,N}\tau_{\mathrm{rep}}\sum_{p=1}^{\infty}\frac{1}{p^2(p^2+\tau_{\mathrm{rep}}\tau_c^{-1}+i\tau_{\mathrm{rep}}\omega)}\ (p\ \text{odd})=\frac{8}{\pi^2}G_{0,N}\tau_{\mathrm{rep}}S_{\mathrm{rep}}. \tag{A23}$$

Define the integration contour as in Fig. 8 with β is taken to approach infinity. Replace the fixed number N by a variable integer m, which also approaches infinity, and use the integration contour C_{inf}. We evaluate S_{rep} from the contour integral,

$$I=\oint_{C_{\mathrm{inf}}}\frac{\tan(\pi z/2)dz}{z^2(z^2+\tau_{\mathrm{rep}}\tau_c^{-1}+i\tau_{\mathrm{rep}}\omega)}=\oint_{C_{\mathrm{inf}}}F(z)dz. \tag{A24}$$

The integrations along the horizontal and the vertical portions of C_{inf} vanish as $\beta\to+\infty$ and/or as $m+\alpha\to+\infty$ since the auxiliary function $F(z)$ approaches zero.

On the other hand, $F(z)$ has simple poles at $z=0,\pm1,\pm3,\ldots,\pm p,\ldots$ (odd numbers) and $z=\pm i\sqrt{\tau_{\mathrm{rep}}\tau_c^{-1}+i\tau_{\mathrm{rep}}\omega}$, all lying within the contour C_{inf}: Application of the residual theorem to Eq. (A24) yields after rearrangement,

$$\sum_{p=1}^{\infty}\mathrm{Res}\{F(z),z=\pm p\}+\mathrm{Res}\{F(z),z=0\}+\mathrm{Res}\{F(z),z=\pm i\sqrt{\tau_{\mathrm{rep}}\tau_c^{-1}+i\tau_{\mathrm{rep}}\omega}\}=0. \tag{A25}$$

The residues for $p=\pm1,\ldots,\pm N$ are

$$\mathrm{Res}\{F(z),z=\pm p:\mathrm{odd}\}=-\frac{2}{\pi}\frac{1}{p^2(p^2+\tau_{\mathrm{rep}}\tau_c^{-1}+i\tau_{\mathrm{rep}}\omega)}, \tag{A26}$$

for $p=0$ the residue is

$$\mathrm{Res}\{F(z),z=0\}=\frac{\pi}{2}\frac{1}{\tau_{\mathrm{rep}}\tau_c^{-1}+i\tau_{\mathrm{rep}}\omega}, \tag{A27}$$

while the last two residues are

$$\mathrm{Res}\{F(z),z=\pm i\sqrt{\tau_{\mathrm{rep}}\tau_c^{-1}+i\tau_{\mathrm{rep}}\omega}\}=-\frac{1}{2}\frac{\tanh(\pi/2\sqrt{\tau_{\mathrm{rep}}\tau_c^{-1}+i\tau_{\mathrm{rep}}\omega})}{(\tau_{\mathrm{rep}}\tau_c^{-1}+i\tau_{\mathrm{rep}}\omega)^{3/2}}. \tag{A28}$$

Hence, after substitution into Eq. (A25), we have the exact result for the sum

$$-(4/\pi)S_{\mathrm{rep}}+\frac{\pi}{2}\frac{1}{\tau_{\mathrm{rep}}\tau_c^{-1}+i\tau_{\mathrm{rep}}\omega}-\frac{\tanh(\pi/2\sqrt{\tau_{\mathrm{rep}}\tau_c^{-1}+i\tau_{\mathrm{rep}}\omega})}{(\tau_{\mathrm{rep}}\tau_c^{-1}+i\tau_{\mathrm{rep}}\omega)^{3/2}}=0. \tag{A29}$$

Substituting S_{rep} into Eq. (A23) produces the expression for the contribution from chains of length N to the complex viscosity for living polymers whose dynamics is described by the reptation model with chemical relaxation. Thus, the contribution to the viscoelastic function from chains of length N is

$$\eta_{c,N}^*(\omega)=G_{0,N}\left[\frac{1}{\tau_c^{-1}+i\omega}-\frac{2}{\pi}\frac{\tanh(\pi/2\sqrt{\tau_{\mathrm{rep}}\tau_c^{-1}+i\tau_{\mathrm{rep}}\omega})}{\tau_{\mathrm{rep}}^{1/2}(\tau_c^{-1}+i\omega)^{3/2}}\right]. \tag{A30}$$

The average viscosity is given by integration over the equilibrium mass distribution, namely,

$$\eta_c^*(\omega)=\int_0^{\infty}dNNc_N\eta_{c,N}^*(\omega), \tag{A31}$$

with N-dependent characteristic times for chemical reaction of assembly-disassembly τ_c and structural rearrangement of the chain τ_{rep}, respectively. The dependence of τ_c on the chain length is considered in Sec. II D, while the scaling of the reptation time τ_{rep} with N is discussed briefly in the comments after Eq. (44).

For infinitely long $\tau_c\to\infty$, we recover the viscosity for the reptation model in the absence of chemical relaxation. The contribution from chains of fixed length N is obtained in this limit as

$$\eta_N^*(\omega) = G_{0,N}\left[\frac{1}{i\omega} - \frac{2}{\pi}\frac{(-1)^{3/4}\tan(\pi/2(-1)^{3/4}(\tau_{\rm rep}\omega)^{1/2})}{\tau_{\rm rep}^{1/2}\omega^{3/2}}\right], \tag{A32}$$

by setting $\tau_c^{-1} \to 0$ and using simple algebra transformations. The real and imaginary components of $\eta_N^*(\omega)$ are given by

$$\eta_N'(\omega) = \frac{\sqrt{2}}{\pi}\frac{G_{0,N}}{\tau_{\rm rep}^{1/2}\omega^{3/2}} \times\left[\frac{\tanh\alpha(1+\tan^2\alpha) - \tan\alpha(1-\tanh^2\alpha)}{1+\tanh^2\alpha\tan^2\alpha}\right], \tag{A33}$$

$$\eta_N''(\omega) = G_{0,N}\left\{\frac{1}{\omega} - \frac{\sqrt{2}}{\pi}\frac{1}{\tau_{\rm rep}^{1/2}\omega^{3/2}} \times\left[\frac{\tanh\alpha(1+\tan^2\alpha) + \tan\alpha(1-\tanh^2\alpha)}{1+\tanh^2\alpha\tan^2\alpha}\right]\right\},$$

where

$$\alpha = \frac{\pi}{2}\left(\frac{\tau_{\rm rep}\omega}{2}\right)^{1/2}. \tag{A34}$$

The zero-shear viscosity $\eta_{0,N} = \eta_N^*(0)$ in the reptation model may be found by contour integration. However, $\eta_N^*(0)$ may also be obtained from Eq. (A33) by expanding $\eta_N'(\omega)$ about $\omega = 0$. Since $\tan\alpha = \alpha + \frac{1}{3}\alpha^3 + \bar{o}(\alpha^4)$ and $\tanh\alpha = \alpha - \frac{1}{3}\alpha^3 + \bar{o}(\alpha^4)$ for small α, we have

$$\eta_{0,N} = \frac{\sqrt{2}}{\pi}\frac{G_{0,N}}{\tau_{\rm rep}^{1/2}\omega^{3/2}}\left(\frac{4}{3}\alpha^3\right) = \frac{\pi^2}{12}G_{0,N}\tau_{\rm rep}. \tag{A35}$$

The average over the chain length distribution is evaluated using Eq. (A31) in a similar fashion.

[1] K. Van Workam and J. F. Douglas, Phys. Rev. E **71**, 031502 (2005).
[2] K. Van Workam and J. F. Douglas, Phys. Rev. E **71**, 031502 (2006).
[3] S. C. Greer, J. Phys. Chem. B **102**, 5413 (1998).
[4] J. Zhuang, S. Sakar Das, M. D. Nowakowski, and S. C. Greer, Physica A **244**, 522 (1997).
[5] M. E. Cates and S. J. Candau, J. Phys.: Condens. Matter **2**, 6869 (1990).
[6] M. E. Cates, Europhys. Lett. **4**, 497 (1987).
[7] G. Faivre and J. L. Gardissat, Macromolecules **19**, 1988 (1986).
[8] P. S. Niranjan, P. B. Yim, J. G. Forbes, S. C. Greer, J. Dudowicz, K. F. Freed, and J. F. Douglas, J. Chem. Phys. **119**, 4070 (2003).
[9] S. C. Greer, Annu. Rev. Phys. Chem. **53**, 173 (2002).
[10] S. K. Kumar and J. F. Douglas, Phys. Rev. Lett. **87**, 188301 (2001).
[11] A. V. Tobolsky and A. Eisenberg, J. Am. Chem. Soc. **82**, 289 (1960).
[12] A. Milchev, Y. Rouault, and D. P. Landau, Phys. Rev. E **56**, 1946 (1997).
[13] R. L. Scott, J. Chem. Phys. **69**, 261 (1965).
[14] J. Dudowicz, K. F. Freed, and J. F. Douglas, J. Chem. Phys. **119**, 12645 (2003).
[15] M. Doi and S. F. Edwards, *The Theory of Polymer Dynamics* (Oxford University Press, New York, 1986).
[16] R. E. Rouse, J. Chem. Phys. **21**, 1272 (1953).
[17] M. Mondello, G. S. Grest, E. B. Webb III, and P. Peczak, J. Chem. Phys. **109**, 798 (1998).
[18] M. E. Cates, J. Phys. Chem. **94**, 371 (1990).
[19] C. M. Marques, M. S. Turner, and M. E. Cates, J. Non-Cryst. Solids **172–174**, 1168 (1994).
[20] C. M. Marques, M. S. Turner, and M. E. Cates, J. Chem. Phys. **99**, 7260 (1993).
[21] M. S. Turner and M. E. Cates, J. Phys. (France) **51**, 307 (1990).
[22] J. D. Ferry, *Viscoelastic Properties of Polymers*, 3rd ed. (Wiley, New York, 1980).
[23] F. Lequeux, J. Phys. II **1**, 195 (1991).
[24] Y. N. Kaznessis, D. A. Hill, and E. J. Maginn, J. Chem. Phys. **109**, 5078 (1998).
[25] Y. N. Kaznessis, D. A. Hill, and E. J. Maginn, J. Chem. Phys. **111**, 1325 (1999).
[26] R. Granek and M. E. Cates, J. Chem. Phys. **96**, 4758 (1992).
[27] C. M. Marques and M. E. Cates, J. Phys. II **1**, 489 (1991).
[28] R. B. Blizard, J. Appl. Phys. **22**, 730 (1951).
[29] M. E. Cates, Macromolecules **20**, 2289 (1987).
[30] J. F. Douglas and J. B. Hubbard, Macromolecules **24**, 3163 (1991).
[31] M. S. Turner and M. E. Cates, Langmuir **7**, 1590 (1991).
[32] P. Terech, V. Schaffhauser, P. Maldivi, and J. M. Guenet, Langmuir **8**, 2104 (1992).
[33] S.-Q. Wang and K. F. Freed, J. Chem. Phys. **86**, 3021 (1987).
[34] H. W. Wyld, *Mathematical Methods for Physics* (Benjamin, Reading, MA, 1976).